Journal of Ultrafine Grained and Nanostructured Materials
https://jufgnsm.ut.ac.ir
Vol. 58, No.2, June 2025, pp. 208-218
Print ISSN: 2423-6845 Online ISSN: 2423-6837
DOI: 10.22059/jufgnsm.2025.02.06

# Preparation and Characterization of Poly(PVDF-HFP)–Aluminum Nitride (AlN) Nanocomposite for the Fabrication of Piezoelectric Nanogenerators

***Magesh R, Tamilarasi R, Joelin C, Giftlin George, Rajesh S****

*Department of Applied Physics, Karunya Institute of Technology and Sciences, Coimbatore 641114. Tamil Nadu, India*

*Recieved: 21 August 2025; Accepted: 5 November 2025*

*Corresponding author, E-mail: drsrajesh@karunya.edu

**ABSTRACT**

Flexible piezoelectric nanogenerators (PENGs) are gaining attention as sustainable power sources for wearable and self-powered electronic systems due to their capability to convert mechanical energy into electrical output. The present work aims to enhance the performance of a flexible PENG by incorporating aluminum nitride (AlN) nanoparticles into a poly(vinylidene fluoride-co-hexafluoropropylene) (PVDF-HFP) matrix. The nanocomposite fibers were fabricated through electrospinning technique with an. The structural, morphological, and compositional features were examined using Fourier Transform Infrared Spectroscopy (FT-IR), Energy Dispersive X-ray Spectrometry (EDX), Scanning Electron Microscopy (SEM), and X-ray Diffraction (XRD). FT-IR and XRD analyses confirmed the presence and enhancement of the electroactive β-phase in the composite, while FE-SEM images indicated uniform fiber formation with well-distributed nanoparticles. The optimized device with AlN loading of 15 wt% achieved an output voltage of 2.64 V and a current of 0.49 μA, showing over a tenfold enhancement in voltage and an order of magnitude increase in current compared with pristine PVDF-HFP fibers. The nanogenerator also delivered a power density of 12.00 mW/m² under a 20 MΩ load. These results confirm that AlN nanoparticle incorporation effectively improves dipole alignment and stress transfer, positioning the PVDF-HFP/AlN composite as a strong candidate for high-performance piezoelectric energy harvesting applications.

***Keywords:*** *PENG, AlN, Piezoelectric, PVDF-HFP (Poly Vinylidene Fluoride–Hexa Fluoro Propylene), Aluminum Nitride, Electrospinning.*

## 1. Introduction

Sustainable large-scale technologies for cost-effective energy capture are actively advancing. Energy harvesting is crucial for this process. Nanogenerators offer a promising solution by generating electricity from mechanical or thermal energy without relying on traditional energy storage devices such as batteries. Therefore, there is increasing interest in the field of nanogenerators [1, 2]. To enable widespread commercialization, it is essential to develop nanogenerators using highly efficient, low-cost, and environmentally friendly materials. Additionally, they must have a more favorable environmental impact than other energy harvesting technologies. A viable approach involves utilizing piezoelectric materials to convert vibrational energy into electrical signals. Piezoelectric materials [3] are well matched for converting mechanical stress into electric signals [4]. Certain materials exhibit piezoelectricity, wherein the application of mechanical stress induces the generation of electric charges,

including materials like ZnO [5], PZT [6], $BaTiO_3$ [7] and AlN [8]. Ceramic piezoelectric materials exhibit high piezoelectric coefficients but are often brittle and challenging to process, making them unsuitable for flexible applications. However, with polymer as the host matrix at the micro- or nanoscale, it can enhance the mechanical stability and prevent fractures and structural failures under mechanical stress. In contrast, piezoelectric polymers are lightweight, flexible, nontoxic, and easy to manufacture. PVDF [9] and its copolymers, such as PVDF-HFP [10], exhibit piezoelectric, pyroelectric, and ferroelectric properties, offering diverse structural possibilities when combined with appropriate dielectric materials. Among the various crystalline phases, the electroactive β-phase plays a crucial role in enhancing the piezoelectric properties of PVDF-HFP owing to its strong dipole moment. The composite of ceramic materials and polymers results in an enhanced energy-harvesting device that is characterized by excellent flexibility and improved mechanical strength. To achieve the concept of flexible working nanogenerators [11], fillers are initially added into the polymer matrix, and the prepared material has the combined properties of both the polymer and filler. Fillers such as Lead Zirconate Titanate (PZT) [3], Barium Titanate ($BaTiO_3$) [12,13], aluminum nitride [14, 15], and Titanium Dioxide ($TiO_2$) [9] are used to attain high coefficient values. Among fluoropolymers, PVDF-HFP [16] has gained much attention for PENG devices [17] because of its ease of processing, low cost, great flexibility, and good coefficient values. More fascinating studies have been reported previously based on PENGs with PVDF/$BaTiO_3$ [18] and PVDF/AlN [19] nanocomposites.

Compared with traditional methods for fabricating polymer-piezoelectric ceramic nanocomposites, such as the molten salt technique [20], spin-casting [21] and electrostatic adhesion [22], fiber production techniques [23] that involve stretching and poling at controlled temperatures can significantly improve the β-phase content of PVDF. Electrospinning is an accessible and cost-effective method for producing ultrafine nanofibers with exceptionally high surface-to-volume ratios from a diverse range of polymers and composites. This morphological advantage makes the technology excellent for functionalization and integration of active agents. However, key drawbacks include the low production rate of single-jet systems and a lack of precise control over fiber orientation and pore structure in the final mat. Electrospinning technique involves three primary stages. First, the polymer was mixed with a metal salt sol or inorganic alkoxide, and its viscosity was adjusted to prepare the electrospinning precursor. This precursor was then subjected to electrospinning to form precursor fibers, which were subsequently sintered to obtain the ceramic nanofibers. The key steps in solution electrospinning include charging the solution under an electric field, overcoming the surface tension and viscosity, forming a Taylor cone, and jetting the solution, followed by fiber crystallization and collection. The overall process is influenced by several factors, including environmental conditions, solution characteristics, and operational parameters.

This paper presents the fabrication of flexible films employing a PVDF-HFP polymer and aluminum nitride (AlN) material using an electrospinning technique. This study aims to use the AlN fillers within the PVDF-HFP matrix to enhance piezoelectric performance. The optimization of electrospinning parameters for improved β-phase content and output efficiency and to develop and analyze a flexible piezoelectric nanogenerator (PENG) [24] while exploring its material characteristics and operational mechanism. Aluminum nitride (AlN) was chosen as the active filler due to its excellent chemical stability, corrosion resistance, and durability under harsh conditions, which contribute to longer device lifespan and improved reliability. Its inherent biocompatibility further supports its use in biomedical and wearable energy-harvesting applications. AlN possesses a piezoelectric coefficient of 4.1286 pm/V [25] and a dielectric constant in the range of 8.6–9.0 [26] providing a balanced combination of piezoelectric response, electrical insulation, and thermal conductivity. These advantages, together with its ability to be integrated onto flexible substrates, establish AlN as a highly suitable material for lightweight, compact, and efficient piezoelectric energy-harvesting devices. Electrospun P(VDF-TrFE) nanofibers integrated with lead-free aluminum nitride (AlN) [27] nanoparticles exhibit significantly improved piezoelectric properties. Under perpendicular excitation at 5 Hz and 4 N, the AlN-doped nanofiber membrane (15:0.1) demonstrated a peak open-circuit voltage (Voc) of 106 mV, reflecting a 43% increase, and a short-circuit current (Isc) of 1.1 nA, marking a 50.7% enhancement over the undoped membrane. Structural and morphological evaluations confirmed consistent fiber integrity and enhanced crystallinity with optimal AlN doping (0.1%), achieving a power density of 1.07 $mW/cm^2$. AlN-doped P(VDF-TrFE) nanofiber membranes demonstrated excellent performance in diverse real-time applications such as detecting finger motion, tracking wrist pulse signals, and identifying complex multipoint mechanical actions, highlighting their potential for use in wearable and flexible electronic devices.

## 2. Experimental

### 2.1. Materials

Aluminum nitride (AlN) powder (average particle size ≈10 μm, purity ≥98%), poly(vinylidene fluoride-co-hexafluoropropylene) (PVDF-HFP) pellets (average molecular weight Mw ≈ 400,000 and Mn ≈ 130,000), and N,N-dimethylformamide (DMF, anhydrous, purity 99.8%) were procured from Sigma-Aldrich (USA) and used without any further purification.

### 2.2. Preparation of PVDF-HFP/AlN nanocomposite

A homogeneous solution was prepared by dissolving 1 g of poly(vinylidene fluoride-co-hexafluoropropylene) (PVDF-HFP) in 15 mL of N,N-dimethylformamide (DMF) under continuous stirring overnight. To ensure uniform dispersion of the filler materials, the solution was further stirred for an additional 12 h after introducing aluminum nitride (AlN) powder. The AlN powders were subjected to high-energy ball milling for 2 hours at 400 rpm using zirconia balls prior to incorporation. Subsequently, the milled AlN fillers were added into the PVDF-HFP matrix at concentrations of 5 wt%, 10 wt%, 15 wt%, and 20 wt%. The detailed compositions and sample abbreviations are provided in Table 1.

### 2.3. Electrospinning process

Self-poled piezoelectric polymer fibers were fabricated using electrospinning process demonstrated in figure 1(a). Nanofiber fabrication was performed at different voltage levels to determine the optimal conditions. Among these, 15 kV was found to be the most suitable because it ensured a stable jet, uniform fiber structure, and minimal defects, leading to well-formed nanofibers. The prepared solutions were loaded into a 10 ml syringe equipped with a needle, and the solution was pumped at a precise flow rate of 0.05 ml/hour under a high accelerating voltage of 15 kV. Electrospun fibers were collected on aluminum foil, which acted as the collector and was positioned 10 cm away from the needle tip.

Table. 1- Weight percentages of different prepared composite films

| Sample code | Weight % of PVDF-HFP | Weight % of AlN |
|---|---|---|
| 1E | 100% | |
| 2E | 95% | 5% |
| 3E | 90% | 10% |
| 4E | 85% | 15% |
| 5E | 80% | 20% |

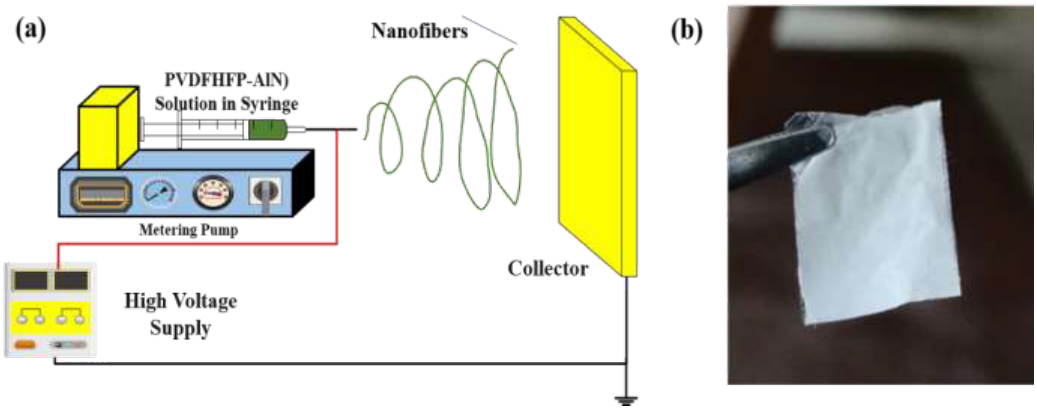


Fig. 1- (a) Schematic illustration of the electrospinning process used for the fabrication of PVDF-HFP/AlN nanofibers, (b) Photograph of the electrospun PVDF-HFP/AlN composite nanofiber film.

### 2.4. PENG Device Fabrication

To evaluate the efficiency of piezoelectric energy generation in electrospun fibers, energy-generating devices were constructed using fibers collected from a stationary collector. The fabrication process involved sandwiching the electrode surface with fibers between two nonconductive tape pieces. Copper wires were securely attached to both electrodes to establish the connectivity. Subsequently, the complete device assembly was fastened onto an insulating plate for characterization. Figure 1(b) illustrates the films created using electrospinning for the fabrication of the device.

### 2.5. Characterization Technique

Surface analysis, including morphological observations and quantitative elemental composition, was conducted using a Scanning Electron Microscope (SEM), the JSM-6390 model manufactured by JEOL Ltd. This unit was equipped with Energy-Dispersive X-ray Spectroscopy (EDS) for comprehensive element mapping. The crystallographic properties—such as structure, size, and lattice strain—were investigated by X-ray diffraction (XRD), utilizing the SHIMADZU XRD-6000 diffractometer from Shimadzu Corporation with Cu-Kα radiation (λ=1.54 A˚). To confirm the successful enhancement of the piezoelectric phase within the nanocomposite, Fourier-transform infrared spectroscopy (FTIR) measurements were performed on a SHIMADZU IRAffinity-1S Spectrophotometer (from Shimadzu Corporation) in Attenuated Total Reflectance (ATR) mode. Finally, the electrical performance of the piezoelectric nanogenerator (PENG) was evaluated by applying pressure via a linear motor. The resulting electrical output was precisely measured using a Keysight InfiniVision DSOX4024A Digital Oscilloscope (manufactured by Keysight Technologies). Voltage signals were captured using a matched Keysight N2894A (10:1) passive probe, and low-noise current measurements were achieved with a Stanford Research Systems SR570 low-noise current amplifier (from Stanford Research Systems).

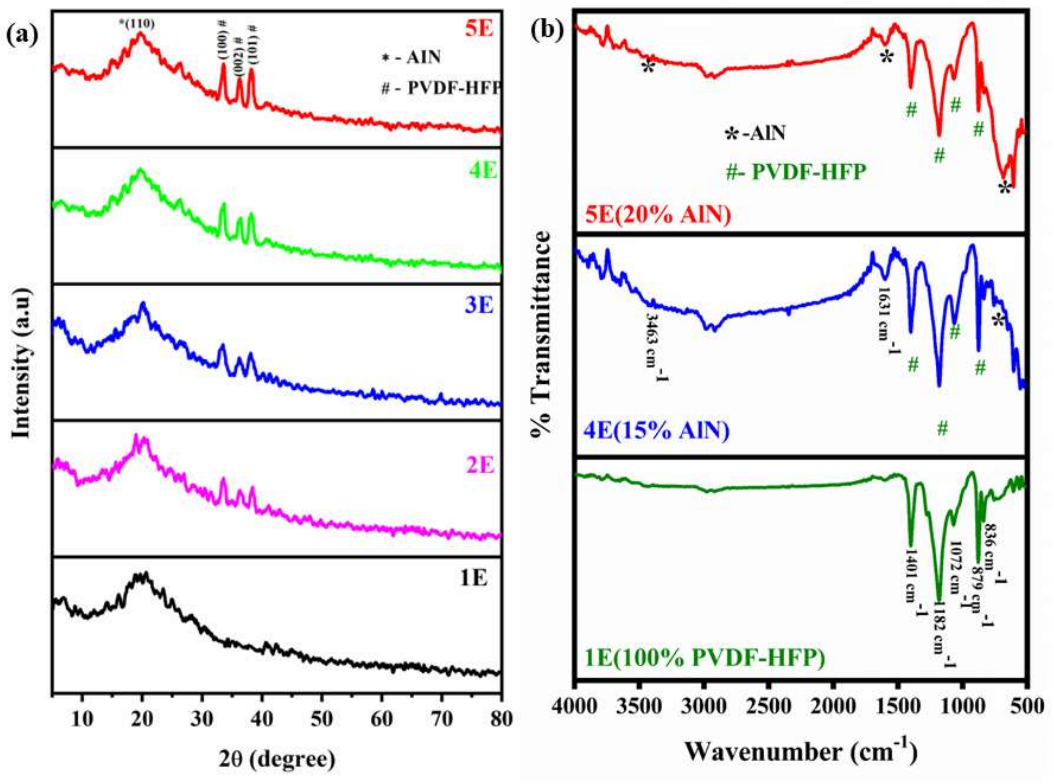


Fig. 2- (a) XRD patterns of the prepared PVDF-HFP/AlN nanocomposite samples—1E (100% PVDF-HFP), 2E (5% AlN), 3E (10% AlN), 4E (15% AlN), and 5E (20% AlN), (b) FTIR spectra of samples 1E (100% PVDF-HFP), 4E (15% AlN), and 5E (20% AlN).

## 3. Results and Discussion

### 3.1. Structural Analysis

Figure 2(a) depicts the X-ray diffraction (XRD) analysis of samples prepared through the electrospinning process at a high-voltage electric field. The results exhibit distinct diffraction peaks of both PVDF-HFP and AlN observed at 20.8°, 33.2°, 36.8°, and 38.4° for the electrospun films with Miller indices of (110), (100), (002), and (101). According to JCPDS Card No. 42-1649, the peak at 20.8° corresponds to the (110) plane of the orthorhombic β-phase of PVDF-HFP. The peaks at 33.2°, 36.8°, and 38.4° are attributed to the (100), (002), and (101) planes of AlN, confirming its hexagonal wurtzite structure as per JCPDS Card No. 25-1133. These findings reveal that the PVDF-HFP and AlN fillers were incorporated together and successfully combined to create a nanocomposite. The presence of these peaks suggested that the PVDF-HFP and AlN fillers were effectively incorporated, forming a uniform nanocomposite material. This incorporation is crucial because it combines the properties of both materials, potentially enhancing the characteristics of the composites.

### 3.2. FTIR Analysis

Functional group analysis of the prepared PVDF-HFP with AlN was performed using Fourier transform infrared (FT-IR) analysis. Figure 2(b) shows the FT-IR spectra of the materials prepared by electrospinning at a high-voltage electric field of 15 kV. These results show the peaks [28] at 836 $cm^{-1}$, $cm^{-1}$,879 $cm^{-1}$,1072 $cm^{-1}$, 1182 $cm^{-1}$, 1273 $cm^{-1}$, and 1401 $cm^{-1}$.The addition of AlN filler shows peaks at 1631 $cm^{-1}$ and 3463 $cm^{-1}$, resulting in $CF_2$ stretching and $CF_2$ wagging, respectively, in the β-phase PVDF crystals. From the above FT-IR data, it was proven that the β phase was formed. This suggests that the crystalline character of PVDF-HFP was not significantly affected by the added AlN compound. The β-phase was calculated using the Beer–Lambert law[23]. It is observed that 1E, 4E, and 5E showed 30.79%, 40.59%, and 54.45%, respectively. The fraction of the β-phase in PVDF-HFP tended to increase as the AlN concentration increased, particularly when the nanocomposite was exposed to high voltage during the electrospinning process.

$$A(\beta) = \frac{A_\beta}{(\frac{K_\beta}{K_\alpha})A_\alpha + A_\beta} \quad (1)$$

where Aβ and Aα denote the absorbance measurements at 841 $cm^{-1}$ and 763 $cm^{-1}$, respectively, and Kα and Kβ are the absorption coefficients at these specific wavenumbers (6.1×104 and 7.7×104×104 $cm^2$ $mol^{-1}$, respectively).

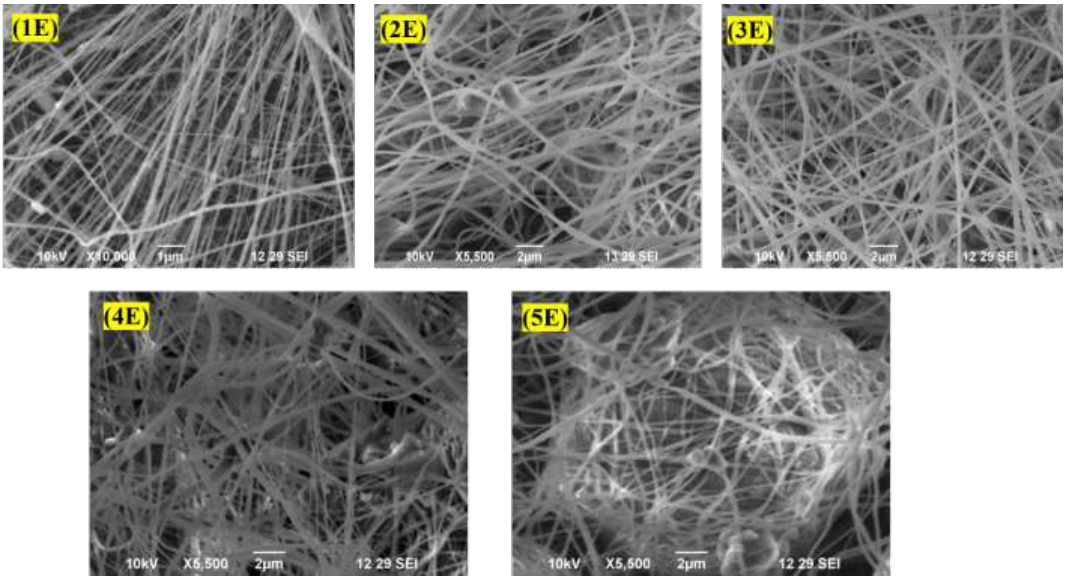


Fig. 3- SEM images of the prepared PVDF-HFP/AlN nanocomposite samples-1E (100% PVDF-HFP), 2E (5% AlN), 3E (10% AlN), 4E (15% AlN), and 5E (20% AlN).

### 3.3. Morphological studies

The surface morphology of the electrospun PVDF-HFP/AlN nanocomposite nanofibers with varying AlN concentrations (0, 5, 10, 15, and 20 wt%) was analyzed using SEM and FESEM techniques, as illustrated in Figure 3. The pure PVDF-HFP sample (1E) exhibited smooth, uniform, and bead-free nanofibers, confirming proper jet stability and continuous fiber formation during electrospinning. Upon the incorporation of AlN nanoparticles, noticeable morphological variations were observed. At lower filler contents (5 and 10 wt%), the nanofibers maintained uniformity and good dispersion of nanoparticles, while at higher concentrations (15 and 20 wt%), the fibers appeared irregular and twisted due to increased solution viscosity and nanoparticle agglomeration.

The FE-SEM morphology of the film 1E (100% PVDF-HFP) shown in Figure 4 confirms the successful formation of uniform nanofibers. The corresponding EDAX spectrum for sample 1E displays distinct peaks for carbon (C) and fluorine (F), verifying the presence of the poly(vinylidene fluoride-co-hexafluoropropylene) [PVDF-HFP] polymer. Similarly, the FE-SEM morphology of film 4E presented in Figure 5 reveals the formation of thin, thread-like nanofibers, indicating a well-developed fibrous structure. The EDS analysis of this sample confirms the presence of carbon (C), fluorine (F), aluminum (Al), and nitrogen (N), establishing the incorporation of both aluminum nitride (AlN) and the PVDF-HFP polymer within the composite. The inset table displays the corresponding elemental weight percentages, while the summarized data for samples 1E and 4E are presented in Table 2.

### 4. Electrical studies

Structural analyses revealed that incorporating AlN filler into the PVDF-HFP polymer yielded a composite exhibiting electroactive properties, rendering it suitable for energy-harvesting applications. Films constructed with this composite can efficiently convert mechanical energy into electrical energy. A device was constructed using these films to perform electromechanical measurements of linear motor interactions. Figure 6(a) Schematic representation of the fabrication and working of the PVDF-HFP-AlN piezoelectric nanogenerator (PENG). Figure 6(b) shows the mechanism of the PENG, where the prepared piezoelectric nanogenerator is subjected to mechanical stress or strain, such as bending, stretching, or vibrations, causing the piezoelectric material to deform. This deformation leads to the displacement of the positive and negative charges within the material. Owing to the piezoelectric effect, mechanical deformation causes the positive and negative charges to separate, leading to the accumulation of opposite charges on different surfaces of the piezoelectric material. The separated charges create an electric potential across the material, resulting in the generation of an electrical output that can be measured using appropriate instruments.

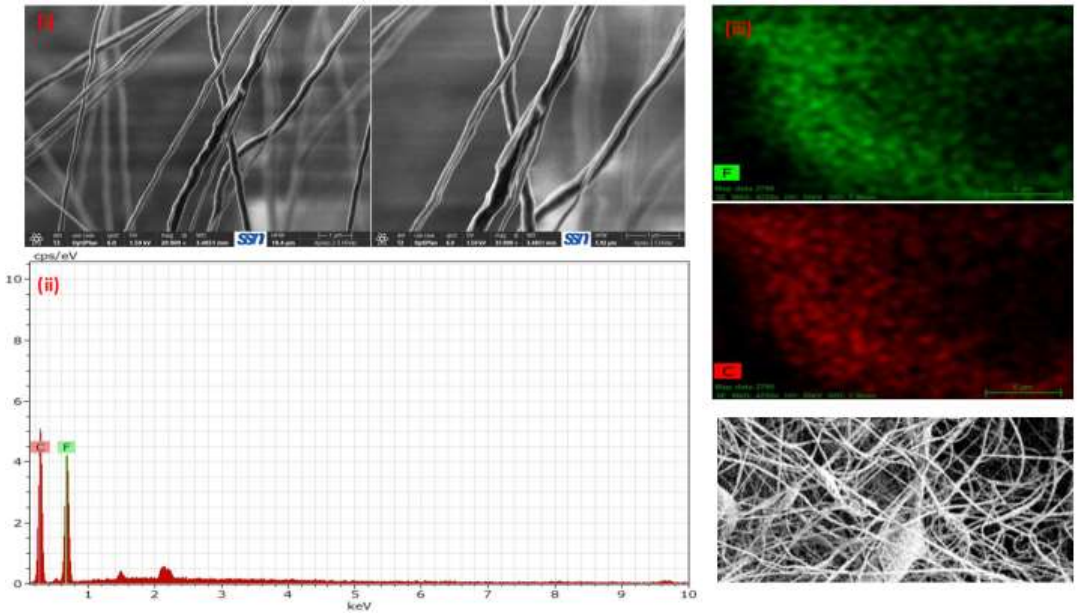


Fig. 4- (i) FESEM image of pure PVDF-HFP nanofibers (sample 1E); (ii) EDX spectrum confirming the elemental composition of the PVDF-HFP sample; (iii) Elemental mapping of the selected region, indicating homogeneous element distribution within the nanofiber structure.

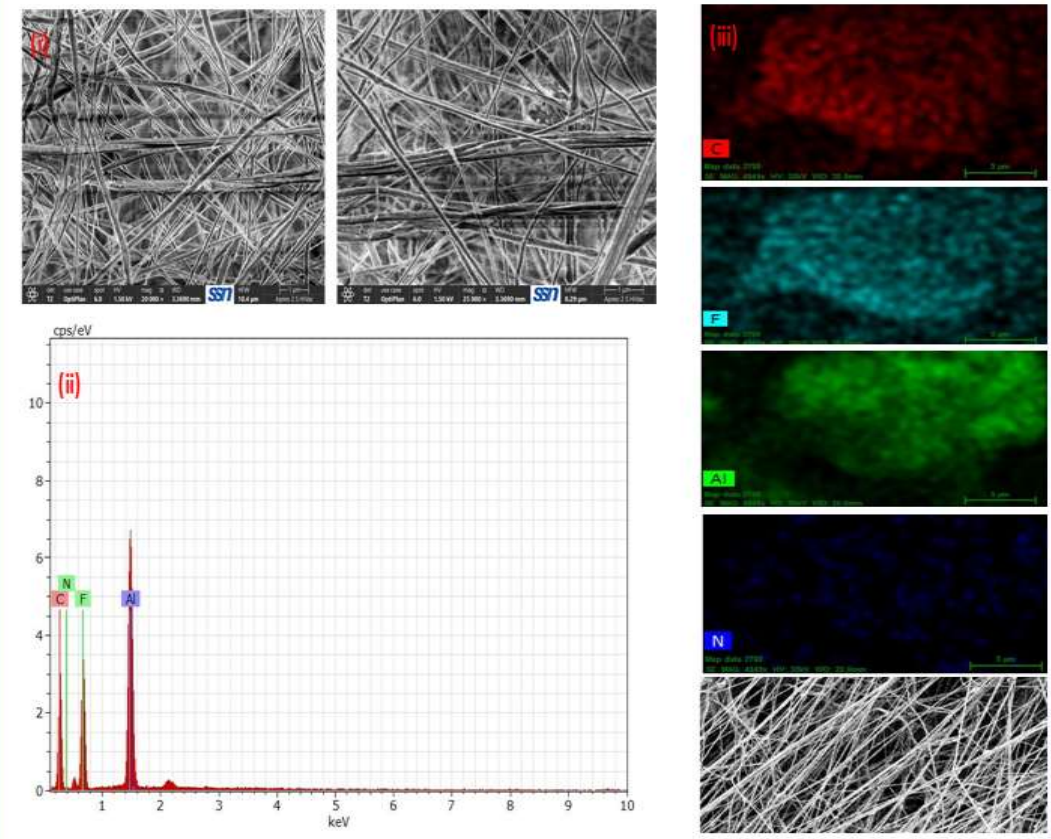


Fig. 5- (i) FESEM image of the PVDF-HFP/AlN nanocomposite (sample 4E, 15% AlN) showing well-formed, interconnected nanofibers; (ii) EDX spectra confirm the presence of Al and N elements in the composite; (iii) Elemental mapping of the selected area, demonstrating uniform dispersion of AlN nanoparticles throughout the polymer matrix.

Table. 2- Quantitative elemental composition (wt%) of the electrospun samples 1E and 4E, as determined by Energy-Dispersive X-ray Spectroscopy (EDS)

| Sample code | Elements present | Weight Percentage (wt%) |
|---|---|---|
| 1E (100% PVDF-HFP) | Carbon (C) | 60.8 |
| | Fluorine (F) | 39.19 |
| 4E(PVDF-HFP-AlN) nanocomposite | Carbon (C) | 51.67 |
| | Fluorine (F) | 31.22 |
| | Aluminum (Al) | 6.57 |
| | Nitrogen (N) | 5.43 |

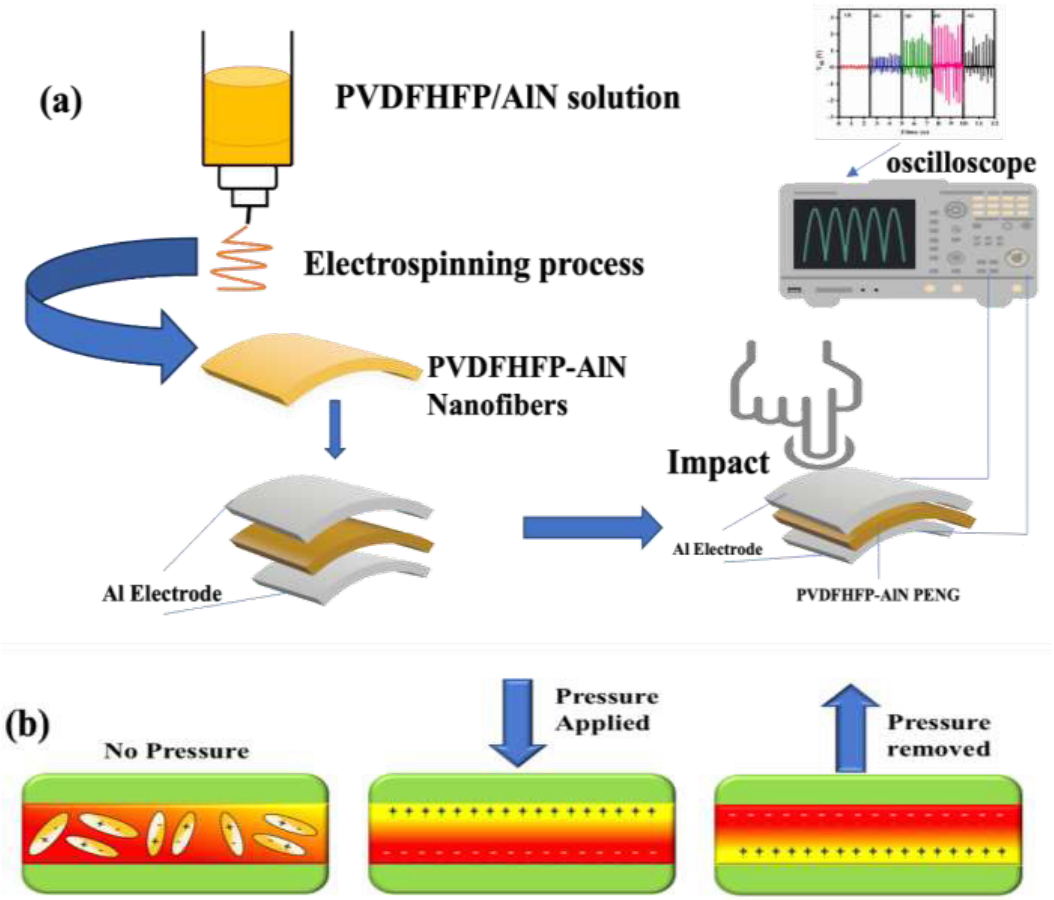


Fig. 6- (a) Schematic illustration of the fabrication and working mechanism of the PVDFHFP-AlN piezoelectric nanogenerator (PENG), (b) Mechanism of PENG, the device's default setting,
No Pressure: When mechanical stress is applied, the dipole moments in the piezoelectric material are randomly oriented, resulting in a neutral charge and no voltage generation.
Pressure Applied: Mechanical pressure deforms the crystal lattice of the material, aligning the dipoles and creating an organized charge distribution. This generates electric charge on the surface and produces a measurable voltage.
Pressure Removed: When pressure is released, the material returns to its original state, the dipoles realign, and the surface charges disappear, restoring a neutral charge state.

Table. 3- Comparison Chart Showing the Previous Reports on the Piezoelectric Output Performance

| S.No. | Piezoelectric material | Method of preparation | Output Voltage (V) | Output Current (μA) | Reference |
|---|---|---|---|---|---|
| 1 | PVDF-$BaTiO_3$ | Solvent Evaporation process and poling | 7.2 | - | [29] |
| 2 | PVDFHFP-$BaTiO_3$ | Electrospinning | ~7.7V | 0.77 | [23], [30] |
| 3 | (PVDFTrFE)/AlN – Perpendicular excitation method | Electrospinning | 0.1 | 0.0011 | [27] |
| 4 | (PVDFTrFE)/AlN – Transverse excitation method | Electrospinning | 82.1 | 2.0 | [27] |
| 5 | AlN/Kapton, Mo | Sputtering | 5.5 | - | [19] |
| 6 | AlN | DC Sputtering | 0.7 | - | [15] |
| 7 | PVDF-AlN | Electrospinning | 2.7 | 0.44 | This work |

When mechanical stress is applied by pressing or bending, the composite undergoes deformation. This causes the beta-phase dipoles in the PVDF-HFP to realign, resulting in a charge imbalance. Simultaneously, the strained AlN particles generate their own piezoelectric charges. The combined effects of these responses enhance the overall voltage and current output. The generated electrical energy was then measured. Table 3 shows the piezoelectric output performance of various PENG devices prepared using different piezoelectric materials and coating techniques.

Fabricated electrospun film samples (2 cm × 2 cm) were cut and sandwiched between two aluminum electrodes for electrical connection. When stress is applied, the samples undergo mechanical deformation and provide an output voltage, which is actually the reverse-piezoelectricity. When the stress is released, the built-in potential decreases with the mechanical deformation's recession and gives a negative potential in the opposite direction. Finally, both peak-to-peak voltages generated can be recorded by connecting an electrometer. The instrument was nullified before sample measurement to avoid any external output caused by friction. Electrospun nanofiber samples had the highest voltage: 2.64 V for sample 4E, 0.15 V for sample 1E (pure PVDF-HFP), 0.84 V for sample 2E, 2.01 V for sample 3E, and 1.98 V for sample 5EB. From the findings, it was shown that for the electrospun samples, the output voltage increased with the AlN filler concentration in the nanocomposite, as shown in figure 7(a).

As the Aluminum Nitride (AlN) concentration increases, the samples agglomerate, and the materials deteriorate the agglomerated particles, which can interfere with the polymer matrix, creating structural inconsistencies that weaken the stress transfer. As a result, mechanical energy conversion into electrical energy becomes less efficient owing to the non-uniform composition of the composite. Because of that, there is no increase in output voltage Thus, it is concluded that AlN filler has outstanding piezoelectric characteristics and can be used to build effective flexible PENG devices.

Among the electrospun nanofiber samples, sample 4E exhibited the highest output current of 0.49 μA, followed by sample 3E (0.30 μA), sample 5E (0.25 μA), sample 2E (0.16 μA), and sample 1E (pure PVDF-HFP) with the lowest current of 0.045 μA. which is shown in figure 7(b). An analysis of these results suggests a trend in which increasing filler concentration correlates with higher current values. Notably, sample 4E showcased the most robust output current, recording 0.49 (μA), while sample 2E came in second with 0.30 (μA) However, beyond

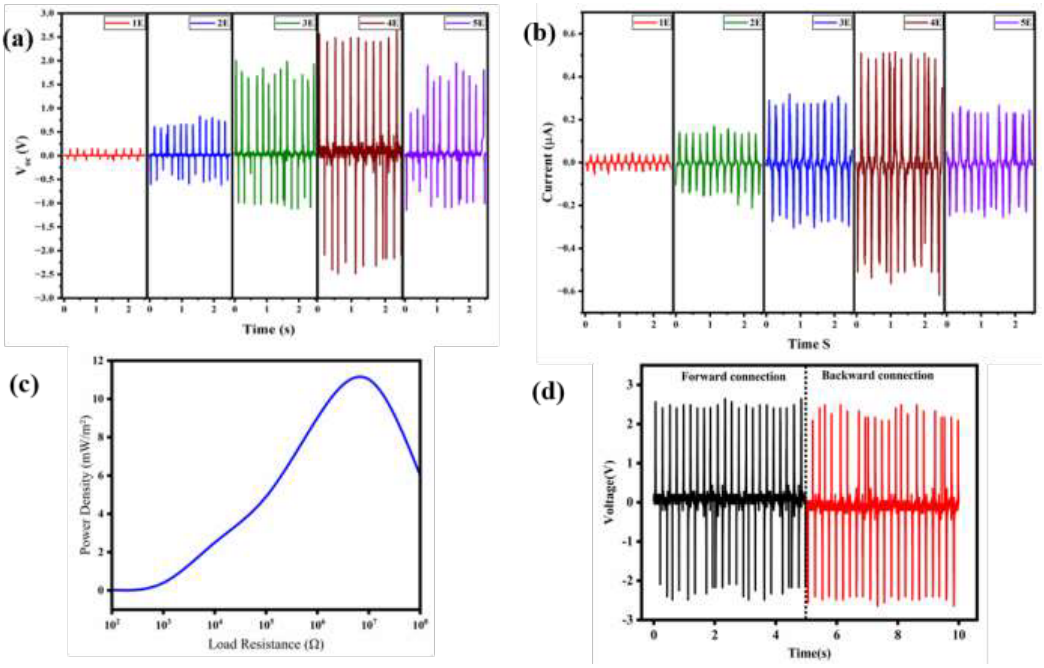


Fig. 7- (a) Output voltage characteristics of PVDF-HFP/AlN nanogenerators with varying AlN concentrations (samples 1E to 5E), (b) Output current characteristics of PVDF-HFP/AlN nanogenerators with varying AlN concentrations (samples 1E to 5E), (c) The maximum power density of the PVDF-HFP/AlN nanogenerator is measured at different load resistances, (d) A polarity test validates the piezoelectric nature and directional dependence of the PVDF-HFP/ AlN PENG device.

a certain threshold of filler content, agglomeration phenomena become apparent, leading to decreased current outputs. This phenomenon is observed in sample 5E, which demonstrated a lower current of 0.25 μA, respectively. Figure 7(c) illustrates the variation in power density with respect to load resistance. As the load resistance increased, the power density followed an upward trend, reaching a peak of approximately $10^6$ MΩ. Beyond this optimal resistance, the power density began to decrease. This behavior is typical in energy-harvesting systems, where the maximum power transfer occurs at a specific resistance. When the resistance was too high, the voltage increased, but the corresponding current decreased significantly, leading to a reduced power output. The maximum power density of the prepared device was determined using the formula $P=I^2R/A$, where P is the power density, I is the current, R is the external load resistance, and A is the area. The device exhibited a peak power density of 12.00 mW/m² at a load resistance of 20 MΩ. Figure 7(d) compares the voltage signals during forward and backward connections, highlighting the device response to polarity changes, with the black waveform representing the forward connection and the red waveform showing the reversed connection. This confirms the piezoelectric nature of the device, as polarity reversal is a characteristic feature of piezoelectric materials.

Figure 8 shows the electrical performance of the AlN-PVDF-HFP-based nanogenerator, emphasizing its voltage generation under specific conditions. Part a) Stability assessment was performed on the fabricated device by applying pressure. presents a voltage-time graph over an extended period, 0 to 2500 seconds, with voltage ranging between -2.5 V and 2.5 V, demonstrating consistent and stable output, with inset graphs providing a closer look at voltage fluctuations during particular operational phases. Part b) Part b) Stability assessment was performed on the fabricated device by applying pressure. presents a voltage-time graph over an extended period, 0 to 2500 seconds, with voltage ranging between -2.5 V and 2.5 V, demonstrating consistent and stable output, with inset graphs providing a closer look at voltage fluctuations during particular operational phases. Part (c) The rectified voltage section of the graph illustrates a stabilizing trend around 0 to 2 volts over a 5-second interval, demonstrating the device's ability to adapt to varying mechanical inputs, which is crucial for applications requiring uniform energy delivery. Part (d) includes a real-time photograph of the experimental setup, where the nanogenerator powers LEDs, along with a schematic diagram illustrating its structural layers and the direction of the applied mechanical pressure. Together, these results highlight the ability of the nanogenerator to reliably convert mechanical energy into electrical energy, making it a promising candidate for energy harvesting applications in wearable electronics, sensors, and self-powered devices.

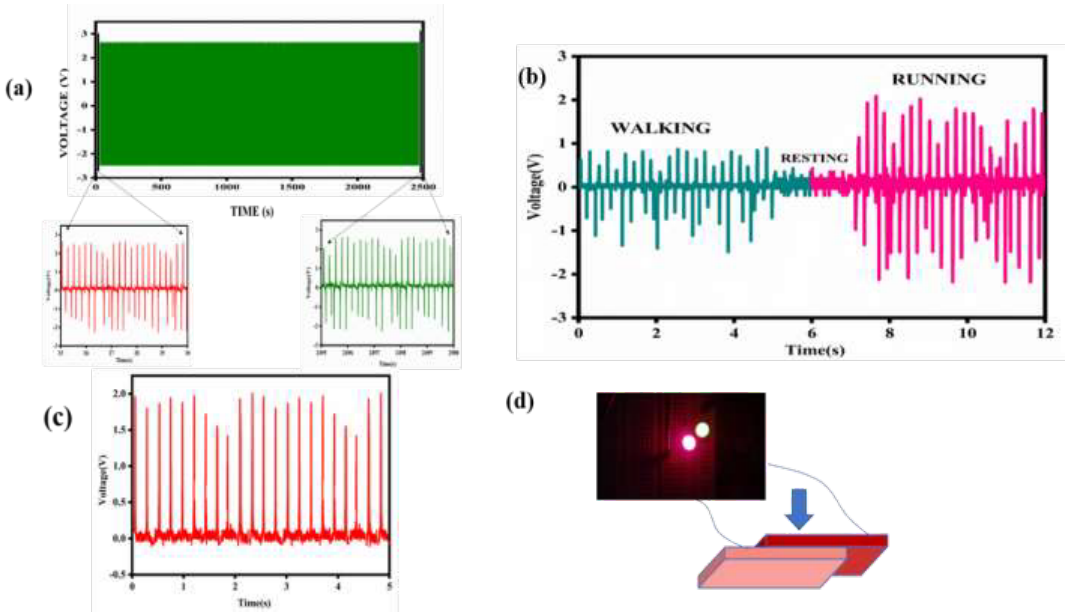


Fig. 8- (a) Stability performance of the PVDF-HFP/AlN PENG device, (b) Output voltage generated when integrated into a shoe sole Stability performance of the PVDF-HFP/AlN PENG device, (c) Rectified voltage of the PVDF-HFP/AlN nanogenerator, (d) Illumination of LEDs under repeated mechanical pressure.

## 5. Conclusion

This study successfully demonstrates the fabrication of flexible piezoelectric nanogenerators (PENGs) based on electrospun PVDF-HFP/AlN nanocomposites for efficient mechanical energy harvesting. The electrospinning process enabled the formation of aligned, well-distributed nanofibers with enhanced effective surface area, enhancing strain sensitivity and flexibility, while the high-voltage field induced self-poling, eliminating the need for external poling. The incorporation of aluminum nitride (AlN) nanoparticles promoted the formation of the electroactive β-phase in PVDF-HFP, improving dipole alignment and piezoelectric response. A systematic increase in AlN content showed a positive correlation with output performance, with the 15 wt% AlN (sample 4E) exhibiting the best results, achieving a peak voltage of 2.64 V and a maximum current of 0.47 μA at 15 kV. The device also delivered a maximum power density of 12.0 mW/m² under a load resistance of 20 MΩ, confirming its effective energy conversion capability. During mechanical motion, the nanogenerator produced stable voltage outputs of 0–1 V during walking and up to 2 V during running, maintaining consistent performance over 2500 seconds with voltages between –2.5 V and 2.5 V. The ability to power LED lights further demonstrated its practical potential for motion-based energy harvesting. Overall, this work highlights that the inclusion of AlN fillers significantly enhances the piezoelectric and electrical performance of PVDF-HFP composites, which is helpful in optimizing filler concentration and processing parameters toward the development of next-generation flexible and efficient nanogenerators for self-powered electronic applications.

## References


1. Briscoe J, Dunn S. Piezoelectric nanogenerators – a review of nanostructured piezoelectric energy harvesters. Nano Energy. 2014;14:15–29.
2. Gaur A, Kumar C, Tiwari S, Maiti P. Efficient energy harvesting using processed poly(vinylidene fluoride) nanogenerator. ACS Appl Energy Mater. 2018;1(7):3019–3024.
3. Anton SR, Sodano HA. A review of power harvesting using piezoelectric materials (2003–2006). Smart Mater Struct. 2007;16(3).
4. Gaur A, Kumar C, Shukla R, Maiti P. Induced piezoelectricity in poly(vinylidene fluoride) hybrid as efficient energy harvester. ChemistrySelect. 2017;2(27):8278–8287.
5. Jana S, Garain S, Ghosh SK, Sen S, Mandal D. γ-Crystalline non-electrically poled photoluminescent ZnO–PVDF nanocomposite film for wearable nanogenerators. Nanotechnology. 2016;27(44):1–12.
6. Chen X, Xu S, Yao N, Shi Y. 1.6 V nanogenerator for mechanical energy harvesting using PZT nanofibers. Nano Lett. 2010;10(6):2133–2137.
7. Hussein AD, Sabry RS, Abdul Azeez Dakhil O, Bagherzadeh R. Effect of adding BaTiO3 to PVDF as nanogenerator. J Phys Conf Ser. 2019;1294(2).
8. Guido F, Qualtieri A, Algieri L, Lemma ED, De Vittorio M, Todaro MT. AlN-based flexible piezoelectric skin for energy harvesting from human motion. Microelectron Eng. 2016;159:174–178.
9. Gowdaman R, Deepa A, Singla YK. Recent advances in PVDF/carbon-based nanocomposite fibers for piezoelectric energy harvesting applications. J Electron Mater. 2024;54(1):24–50.
10. Shanmugaraj P, Swaminathan A, Ravi RK, Dasaiah M, Senthil Kumar P, Sakunthala A. Porous PVDF-HFP/graphene oxide composite membranes prepared by solution casting technique. J Mater Sci Mater Electron. 2019;30(22):20079–20087.
11. Zhang C, Fan W, Wang S, Wang Q, Zhang Y, Dong K. Recent progress of wearable piezoelectric nanogenerators. ACS Appl Electron Mater. 2021;3(6):2449–2467.
12. Athira BS, George A, Vaishna Priya K, Hareesh US, Gowd EB, Surendran KP, Chandran A. High-performance flexible piezoelectric nanogenerator based on electrospun PVDF–BaTiO3 nanofibers for self-powered vibration sensing applications. ACS Appl Mater Interfaces. 2022.
13. Wang Y, Zhang X, Guo X, Li D, Cui B, Wu K, Yun J, Mao J, Xi L, Zuo Y. Hybrid nanogenerator of BaTiO3 nanowires and CNTs for harvesting energy. J Mater Sci. 2018;53(18):13081–13089.
14. Yang J, Xu F, Jiang H, Wang C, Li X, Zhang X, Zhu G. Piezoelectric enhancement of electrospun AlN-doped P(VDF-TrFE) nanofiber membrane. Mater Chem Front. 2021;5(15):5679–5688.
15. Kulkarni ND, Kumari P. Highly flexible PVDF–TiO2 nanocomposites for piezoelectric nanogenerator applications. Mater Res Bull. 2023;157:112039.
16. Kashyap DK, Srivastava AK, Gupta MK. Lightweight, self-poled, flexible piezoelectric tungsten disulfide quantum dots-reinforced PVDF-HFP nanogenerator. ACS Appl Electron Mater. 2023.
17. Wang Y, Fang M, Tian B, Xiang P, Zhong N, Lin H, Luo C, Peng H, Duan CG. Transparent PVDF-TrFE/graphene oxide ultrathin films with enhanced energy harvesting performance. ChemistrySelect. 2017;2(26):7951–7955.
18. Zhao Y, Liao Q, Zhang G, Zhang Z, Liang Q, Liao X, Zhang Y. High-output piezoelectric nanocomposite generators composed of oriented BaTiO3 nanoparticles in PVDF. Nano Energy. 2015;11:719–727.
19. Phatharapeetranun N, Ksapabutr B, Marani D, Bowen JR, Esposito V. 3D-printed barium titanate/poly(vinylidene fluoride) nano-hybrids with anisotropic dielectric properties. J Mater Chem C. 2017;5(47):12430–12440.
20. Mahadeva SK, Walus K, Stoeber B. Piezoelectric paper fabricated via nanostructured barium titanate functionalization of wood cellulose fibers. ACS Appl Mater Interfaces. 2014;6(10):7547–7553.
21. Persano L, Camposeo A, Matino F, Wang R, Natarajan T, Li Q, Pan M, Su Y, Kar-Narayan S, Auricchio F, Scalet G, Bowen C, Wang X, Pisignano D. Advanced materials for energy harvesting and soft robotics: emerging frontiers to enhance piezoelectric performance and functionality. Adv Mater. 2024.
22. Paralı L, Tatardar F, Koç M, Sarı A, Moradi R. Piezoelectric response of electrospun PVDF/PZT incorporated with pristine graphene nanoplatelets for mechanical energy harvesting. J Mater Sci Mater Electron. 2024;35(1):1–15.
23. Kim HJ. Piezoelectric nanogenerator based on lead-free flexible power electronics. 2021.
24. Zhang M, Yang J, Si C, Han G, Zhao Y, Ning J. Piezoelectric properties of AlN thin films for MEMS applications. Micromachines. 2015;6(9):1236–1248.
25. Zientara D, Bućko MM, Lis J. Dielectric properties of aluminium nitride–γ-alon materials. J Eur Ceram Soc. 2007;27(13–15):4051–4054.
26. Joelin C, Praba L, Kuppusamy S, Tamilarasi R, Magesh R, Woong Jung J, Deivasigamani P, Vidhya B, Sakunthala A, Rajesh S. Piezoelectric energy harvesting in PVDF-HFP/BaTiO3 nanofibers and ultrasonic-assisted piezocatalytic degradation of ciprofloxacin. ChemistrySelect. 2024;9(40).
27. Mariello M, Fachechi L, Guido F, De Vittorio M. Multifunctional sub-100 μm flexible piezo/triboelectric hybrid water energy harvester based on biocompatible AlN and parylene-C/PDMS/Ecoflex. Nano Energy. 2021;83:105811.